Inorganic Chemistry

Article

pubs.acs.org/IC

Rational Design of a Ratiometric and Targetable Fluorescent Probe for Imaging Lysosomal Zinc Ions

Lin Xue,[†] Guoping Li,[†,‡] Dongjian Zhu,[†,‡] Qing Liu,[†,‡] and Hua Jiang*[,†]

[†]Beijing National Laboratory for Molecular Sciences, CAS Key Laboratory of Photochemistry, Institute of Chemistry, Chinese Academy of Sciences, Beijing, 100190 P. R. China

[‡]Graduate School of Chinese Academy of Sciences, Beijing, P. R. China

Supporting Information

ABSTRACT: Fluorescent detecting and tracking of zinc ions in living cells has become more and more important because the physiological and pathological functions of zinc are highly associated with the timing and discrete distribution of subcellular zinc ion. For the detection of subcellular zinc concentrations with high spatial and temporal reliability, we report the design, synthesis, properties, and bioimaging evaluation of a fluorescent probe, **DQZn4**, composed of a quinoline scaffold as the ratiometric signaling unit for Zn^{2+} and a dimethylethylamino group as the targeting anchor for lysosomes. In acidic aqueous solution (pH = 5.2), **DQZn4** features fluorescence emission maximum at 542 nm due to the resonance charge transfer in 4-alkoxy substituted quinoline. Upon binding Zn^{2+}, the probe displays significant fluorescent turn-on and ratiometric detection of Zn^{2+} with blue shift of 47 nm and remarkable fluorescence ratio changes ($R = F_{495}/F_{542\ nm}$, R/R_0 = 5.1). Confocal imaging experiments establish that **DQZn4** is able to localize to lysosomes and respond to lysosomal zinc changes in living cells by using fluorescence ratiometry.

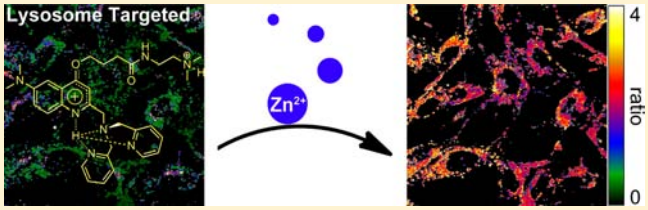

INTRODUCTION

Fluorescence imaging technology, highlighted for the high spatial and temporal resolution, is regarded as a promoting method to monitor biological species in living cells.[1] In recent years, utilizing fluorescence probes to track zinc in subcellular domains has been attracting more and more attention because zinc plays essential roles in many biological processes.[2] Zinc ion not only is a cofactor required for the structure and function of different proteins expressed in the cytoplasm, but also is involved in many organelles including nuclei, mitochondria, endoplasmic reticulum (ER), lysosome, etc.[3] Since the homeostasis of the subcellular zinc is still not well established, visualizing zinc in selected subcellular organelles will help to greatly simplify investigations on zinc network and thus elucidate the mechanisms of zinc physiology.[4] Therefore, it is rather desirable to develop new probes that are able to visualize distribution and concentration of subcellular zinc.

Indeed, targetable probes, usually consisting of a signal reporter and a site-specific tag, such as proteins, peptides, or small chemical markers,[5,6] can be delivered to subcellular domains by targeting tags without interfering distribution of analytes on specific organelles and provide a practical approach to improve subcellular mapping of biospecies. Lysosome is a cytosolic degradative center that contains numerous acidic hydrolases for degradation of all cellular elements. Recent evidence reveals that cellular zinc plays a role in lysosome dysfunction and autophagy/lysosome pathway.[7] The cell death in neurons under oxidative stress has also been linked to lysosome-related zinc dyshomeostasis.[8] Therefore, developing probes for detecting and imaging zinc in lysosomes is a dire need. Up to now, only a few targetable zinc-selective probes are able to localize onto intracellular organelles, including mitochondria, ER, Golgi, and plasma membrane through protein-tags or chemical markers.[9] However, to the best of our knowledge, none of them have yet been realized for lysosomes. Moreover, from the perspective of accurate and quantitative analysis, ratiometric probes have evident advantages compared with the emission intensity-based probes because of their self-calibration via two selected emission wavelengths.[10] Although there has been a huge effort to develop ratiometric Zn^{2+}-selective probes in the past few years,[1,11] the ratiometric and targetable ones are really scarce.[9c,d,h,i]

With these in mind, we take advantage of the versatility of small-molecule sensing unit and targeting tag for subcellular localization to design a new fluorescent probe, **DQZn4**, for detection of lysosomal zinc (Scheme 1). According to our previously reported probes (**DQCd1**, **DQZn1**, and **DQZn2**),[9h,12] the quinoline−DPA (DPA = 2-picolylamine) sensing scaffold, which has been successfully used to design ratiometric probes based on metal-induced inhibition of resonance, is expected to show the following advantages: (i) good stability and water solubility; (ii) high sensitivity toward Zn^{2+} ($K_d \sim$ nM), (iii) high selectivity over Na^+, K^+, Ca^{2+}, and Mg^{2+}, (iv) protonation at neutral aqueous media to emit

Received: June 20, 2012
Published: September 27, 2012

Scheme 1. Design of DQZn3 and DQZn4

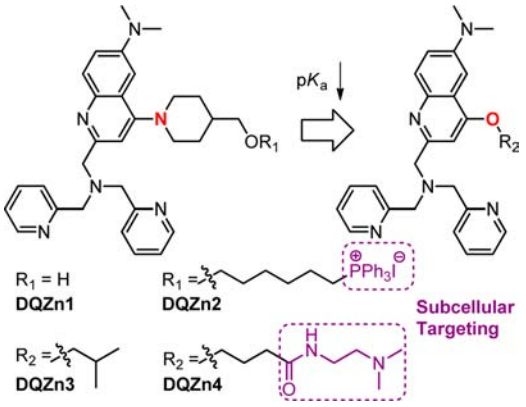

apparent fluorescence due to the resonance charge transfer, and (v) remarkable blue-shift in fluorescence wavelength (>40 nm) in response to Zn^{2+} for ratiometric measurements. We envisioned that the displacement of the nitrogen atom with oxygen atom is expected to weaken the resonance charge transfer from the 4-position electron-donating atom to the quinolinic nitrogen atom (Scheme 1), so that the probe would have smaller pK_a value and exhibit stronger fluorescence emission under acidic conditions than that under neutral conditions. The attachment of a basic dimethylethylamino moiety, as the lysosome anchor, to the tail of the 4-position on quinoline fluorophore would cause the accumulation of the probe in the acidic vesicles, because of the protonation of the dimethylethylamino moiety.[6b,c,f] Meanwhile, the intrinsic photophysical properties of the sensing moiety are not much affected by the lysosome anchor. To evaluate our design, a control molecule **DQZn3**, in which the dimethylethylamino moiety was displaced with an isobutyl group, was also prepared (Scheme 2).

RESULTS AND DISCUSSION

Synthesis. The synthetic strategies for preparing probes are outlined in Scheme 2. **DQZn3** and compound **12** were easily prepared according to the reported procedures.[9h,13] Saponification of **12** can give the carboxylic acid in a quantitative yield, which was further treated with oxalyl chloride, and subsequently reacted with *N*,*N*-dimethylethane-1,2-diamine to obtain **DQZn4** in a reasonable yield.

Protonation Effect on DQZns. Initially, we investigated the effect of pH on the fluorescence properties of **DQZn3** (Figure 1). Two apparent pK_a values of 7.26 ± 0.03 and 4.51 ± 0.03, assignable to the quinolinic nitrogen and one of the 2-pyridyl arms, respectively,[9h,12a] were obtained from the fluorometric data. As expected, the basicity of the quinolinic site is much weaker than that of **DQZn1** (Scheme 1 and Table 1),[9h] in which a nitrogen atom occupies the 4-position of quinoline. The decrease of basicity can be interpreted by the weaker electron-donating ability of an oxygen atom that affords the resonance charge transfer. Meanwhile, two similar pK_a

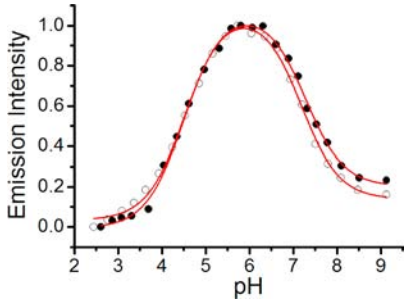

Figure 1. Effect of pH on normalized emission intensity of 5 μM **DQZn3** (●, λ_{em} = 540 nm) and **DQZn4** (○, λ_{em} = 542 nm) in aqueous solutions, λ_{ex} = 405 nm. The solid lines represent the nonlinear least-squares fits to the experimental data.

Scheme 2. Synthetic Strategy for DQZn3 and DQZn4

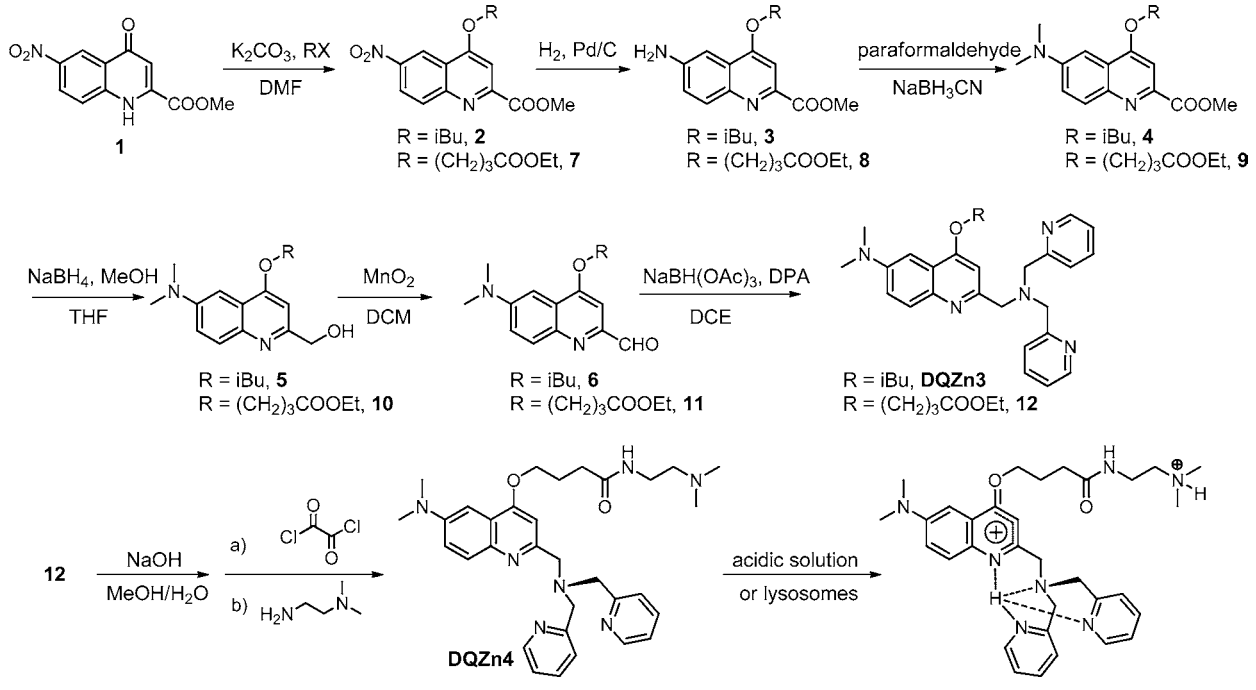

dx.doi.org/10.1021/ic301307v | *Inorg. Chem.* 2012, 51, 10842−10849

Table 1. Spectroscopic Properties of the Probes and Their Zinc Complexes[a]

				$\varepsilon \times 10^3$ (M^{-1} cm^{-1})[b]		λ[nm]$_{em}$[c], Φ	
probe	K_d (nM)	pK_{a1}	pK_{a2}	probe	Zn^{2+} complex	probe	Zn^{2+} complex
DQZn1 (pH = 7.4)[d]	0.54 ± 0.03	8.05 ± 0.02	4.84 ± 0.01	5.90	3.80	550, 0.11	507, 0.15
DQZn2 (pH = 7.4)[d]	0.45 ± 0.01	7.66 ± 0.02	4.57 ± 0.02	5.30	4.10	550, 0.11	504, 0.22
DQZn3 (pH = 7.4)	2.50 ± 0.2	7.26 ± 0.03	4.51 ± 0.03	2.80	2.35	540, 0.10	496, 0.13
DQZn3 (pH = 5.2)	32 ± 2.2			4.30	1.50	540, 0.09	500, 0.10
DQZn4 (pH = 7.4)	0.2 ± 0.01	7.19 ± 0.03	4.52 ± 0.03	1.80	1.80	536, 0.07	495, 0.20
DQZn4 (pH = 5.2)	16 ± 1.1			4.30	1.66	542, 0.11	495, 0.17

[a]10 mM HEPES buffer (pH = 7.4), and 20 mM MES buffer (pH 5.2) were used for measurements. [b]The extinction coefficients were measured at 405 nm. [c]The maximum fluorescence wavelength. [d]See ref 9h.

values of **DQZn4** were also observed to be 7.19 ± 0.03 and 4.52 ± 0.03. No attempt was made to measure the pK_a of the dimethylethylamino moiety because it is a relatively strong base with pK_a of ~10 and is expected to be protonated under weakly basic conditions.[14] Therefore, the dimethylethylamino moiety may cause little PET (photoinduced electron transfer) quenching effect on the fluorescence of **DQZn4** under weakly basic or acidic conditions. Thus, we infer that the attachment of dimethylethylamino moiety does not obviously affect the photophysical properties of **DQZn4** similar to that observed in the case of **DQZn3**. Moreover, the weakly basic quinoline scaffold of **DQZn4** will also contribute to protonation and accumulation in acidic media. Considering the normal pH of lysosomes (4.5−5.5),[15] a MES buffer (20 mM MES, 100 mM NaCl, pH = 5.2) was prepared for photophysical measurements in this context.

Optical Responses of DQZns to Zn^{2+}. The water solubility of **DQZn4** was determined by plotting the fluorescence intensity vs the probe concentration. The data show that **DQZn4** can be dissolved very well in aqueous buffer (20 mM MES, pH = 5.2) (Figure S1). Under these conditions, **DQZn4** exhibited broad absorption around 400−450 nm (ε = 4.3 × 10^3 M^{-1} cm^{-1} at 405 nm) (Figure S2). Coordination of Zn^{2+} caused obvious decrease of this band with several isosbestic points at 268, 299, 320, 344, and 372 nm, which occurred up to 1/1 [Zn^{2+}]/probe ratio, suggesting the formation of 1/1 complex. In the absence of Zn^{2+}, **DQZn4** showed a characteristic emission around 542 nm (Φ = 0.11, Figure 2). Titration of Zn^{2+} resulted in quenching of emission around 543−700 nm and a new blue-shifted emission peak at 495 nm (Φ = 0.17) with a hypsochromic shift of 47 nm and an isoemission point at 543 nm (Table 1). Such sensing properties were very similar to that observed in **DQZn3** (Figure S3), so the significant changes in both absorption and fluorescence spectra could be well explained by the Zn-induced liberation of proton at quinolinic site and subsequent inhibition of resonance.[9h,12] The attachment of dimethylethylamino group on the quinoline scaffold does not exert significant effect on the response of **DQZn4** to Zn^{2+}. In particular, the ratio of emission intensity at 495 and 542 nm increased linearly from 0.37 to 1.88 by titrating of Zn^{2+} until the [Zn^{2+}]/probe ratio reached 1:1, supporting the 1:1 binding stoichiometry as well (Figure 2, inset). By measuring the ratios of emission intensity (F_{495}/$F_{542\ nm}$) at different concentrations of free Zn^{2+} in Zn^{2+}−NTA (NTA = nitrilotriacetic acid) buffered solutions, the dissociation constants (K_d) of **DQZn4** were determined to be 0.2 nM (pH = 7.4) and 16 nM (pH = 5.2), respectively (Figure 3 and S4). We presume that the obviously larger K_d under acidic conditions may result from the competition between the proton and zinc ion. The similar phenomenon was also observed in **DQZn3** (Table 1). It should be noted that the intracellular free Zn^{2+} is usually maintained in extremely low concentration (pM to nM range) by the zinc metalloproteins, whereas the free Zn^{2+} concentration could reach as high as μM level after Zn^{2+} release in response to certain stimulations, such as inflammation and oxidative stress.[3,16] The K_d of 16 nM indicates that **DQZn4** is able to detect Zn^{2+} concentration from nM to μM, which is a suitable range for the release of endogenous Zn^{2+}. Thus, we conclude that **DQZn4** can be an excellent ratiometric fluorescent probe for Zn^{2+} in acidic media.

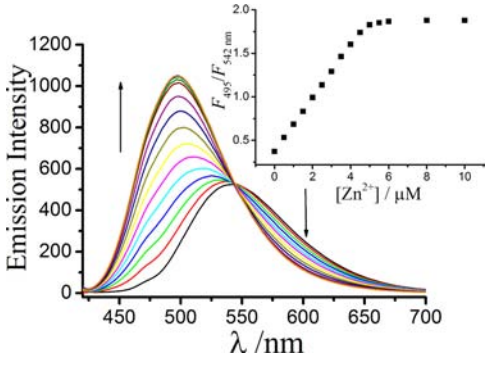

Figure 2. Fluorescence spectra of 5 μM **DQZn4** upon the titration of Zn^{2+} (0−10 μM) in aqueous buffer (20 mM MES, 0.1 M NaCl, pH = 5.2), λ_{ex} = 405 nm. Inset: The emission ratio ($F_{495}/F_{542\ nm}$) changes as a function of Zn^{2+} concentration.

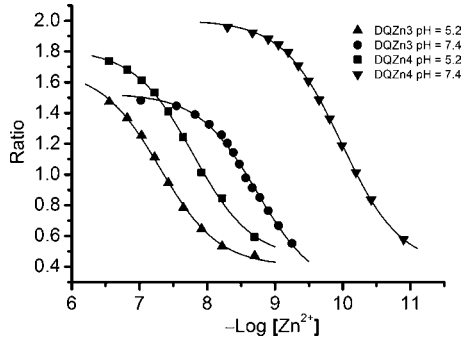

Figure 3. Ratio fluorescence responses of **DQZn3** (▲, $F_{496}/F_{540\ nm}$, pH = 5.2, and ●, $F_{496}/F_{540\ nm}$, pH = 7.4) and **DQZn4** (■, $F_{495}/F_{542\ nm}$, pH = 5.2, and▼, $F_{495}/F_{542\ nm}$, pH = 7.4) as a function of free Zn^{2+} concentration in Zn^{2+}−NTA buffer, λ_{ex} = 405 nm. The solid lines represent the nonlinear least-squares fits to the experimental data.

Generally, introduction of 2-picolylamine (DPA) to quinoline scaffolds can generate highly Zn^{2+}-selective probes under neutral conditions.[17] To evaluate whether this property can be

dx.doi.org/10.1021/ic301307v | Inorg. Chem. 2012, 51, 10842−10849

preserved under acidic conditions, we also measured the response of **DQZn4** to Zn^{2+} in the presence of other metal ions in the MES buffer (pH = 5.2, Figure 4). As expected,

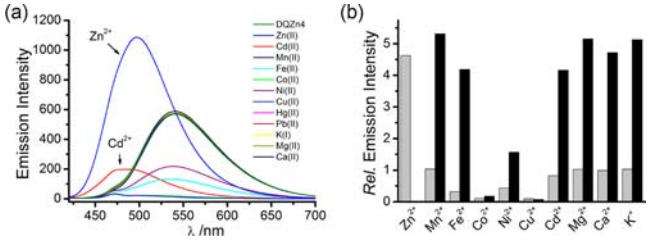

Figure 4. (a) Fluorescence spectra of **DQZn4** (5 μM) in the presence of various metal ions (5 μM Mn^{2+}, Fe^{2+}, Co^{2+}, Ni^{2+}, Cu^{2+}, Zn^{2+}, Cd^{2+}, and 1 mM Mg^{2+}, Ca^{2+}, and K^{+}) in MES buffer (pH = 5.2, λ_{ex} = 405 nm). (b) Selectivity profiles of **DQZn4** (5 μM). Gray bars represent the relative emission intensity (F/F_0, at 495 nm) in the presence of various metal ions. Black bars represent the fluorescence intensity of **DQZn4** in the presence of the indicated metal ions, followed by 5 μM Zn^{2+}.

fluorometric behavior of **DQZn4** was similar to that of **DQZn3** under neutral conditions (Figure S5). **DQZn4** can detect Zn^{2+} with high selectivity over mM-level Na^{+}, K^{+}, Ca^{2+}, Mg^{2+} and 5 μM Mn^{2+}, Fe^{2+} in terms of both emission intensity and ratio calibration. Co^{2+}, Ni^{2+}, and Cu^{2+} also induced obvious ratio response of **DQZn4** but in the manner of quenching the emission (Figure S5). Moreover, they are usually in very low level in living cells with minimum interference with Zn^{2+}. Nonbiological Cd^{2+}, which is a common problem in many Zn^{2+}-selective probes, did not obviously affect zinc-sensing of **DQZn4**. Furthermore, the ratio calibrations of both **DQZn4** and its zinc complex are also pH-insensitive in the acidic condition between pH 4–6 (Figure S6). Therefore, **DQZn4** can be applied to ratiometric detection of Zn^{2+} without the potential influence from other biological metal ions and acidic pH changes.

Ratiometric Fluorescence Imaging of Zn^{2+} in Living Cells. Next, we evaluated the localization properties of **DQZn4** to the acidic compartments in living cells. We stained NIH 3T3 cells with **DQZn4** and LysoTracker Red DND-99, which is a commercially available marker for lysosomes and has good separation in excitation and emission spectra with **DQZn4**. As shown in Figure 5a–c, the pseudocolor images between **DQZn4** and lysotracker overlapped very well, and the Pearson's

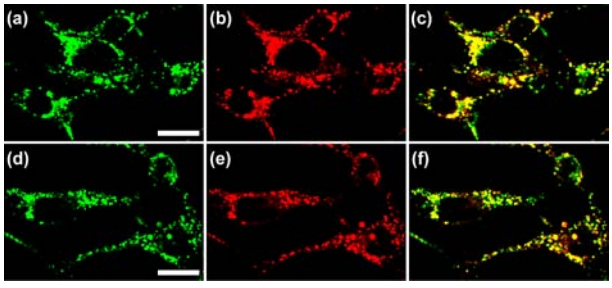

Figure 5. DQZn4 localizes to lysosomes in live NIH 3T3 cells. The cells were stained with (a) 10 μM **DQZn4**, (b) 1 μM LysoTracker Red, (d) 10 μM **DQZn4** and further treated with 30 μM $ZnSO_4$ and 15 μM 2-mercaptopyridine *N*-oxide for 5 min, (e) LysoTracker Red, for 30 min at 37 °C in DMEM. (c) Overlay of (a) and (b), (f) overlay of (d) and (e). Scale bar: 20 μm.

colocalization coefficient, *A*, which describes the correlation of the intensity distribution between the channels to characterize the degree of overlap between images,[18] was measured to be 0.82 by using FV10-ASW software. We further treated the cells with 30 μM $ZnSO_4$ and 15 μM 2-mercaptopyridine *N*-oxide for 5 min to increase the intracellular zinc level. The staining patterns observed from both channels still showed a good overlap with an *A* value of 0.84 (Figure 5d–f). In contrast, the images of the control probe **DQZn3**, which lacked the lysosome anchor, only showed partial overlap with that of Lysotracker with an *A* value of 0.53 (Figure S7). These results demonstrate that dimethylethylamino moiety obviously enhanced the accumulation of **DQZn4** in the acidic lysosomes. Thus, **DQZn4** can be used as a lysosome-specific probe in living cells.

With these data in hand, we applied **DQZn4** to detect zinc in intracellular lysosomes by using single-excitation dual-emission ratiometry. After incubating the NIH 3T3 cells with **DQZn4** (10 μM) for 30 min at 37 °C, **DQZn4** can penetrate through the cell membrane and stain the cells with obvious fluorescence at red emission channel (520–620 nm) and weak fluorescence at green emission channel (430–510 nm) (Figure S8). The ratio calculated as F_{green}/F_{red} gave an average value of 0.43 ± 0.13 (Figure 6e, column a). By treating the cells with 30 μM

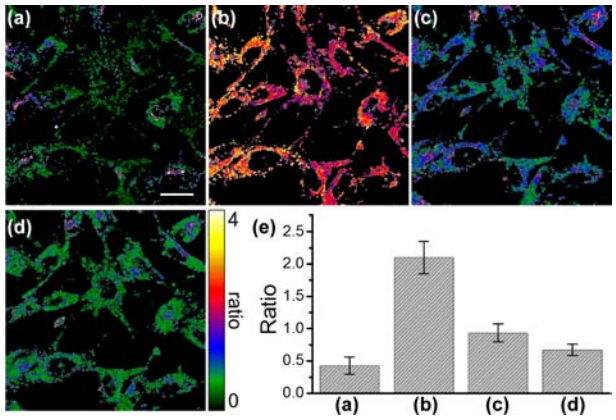

Figure 6. Ratiometric imaging of Zn^{2+} in **DQZn4**-labeled NIH 3T3 cells. (a) Cells were stained with 10 μM **DQZn4** at 37 °C for 30 min. (b) The cells were treated with $ZnSO_4$ (30 μM) and 2-mercaptopyridine *N*-oxide (15 μM) for 5 min. (c, d) These cells were treated with TPEN (50 μM) for 5 and 10 min. (e) Average F_{green}/F_{red} ratios were measured from ten cells in (a–d). λ_{ex} = 405 nm, the ratio (F_{green}/F_{red}) was calculated as $Em_{430-510}/Em_{520-620\ nm}$. Scale bar: 20 μm; ratio bar: 0–4.

$ZnSO_4$ and 15 μM 2-mercaptopyridine *N*-oxide for 5 min, the fluorescence at green channel can be rapidly enhanced. The emission ratio was significantly increased to 2.10 ± 0.25 (Figure 6e, column b). Furthermore, the fluorescence and ratio changes can be gradually reversed by treatment with an excess of TPEN (50 μM; *N*,*N*,*N*′,*N*′-tetrakis(2-pyridylmethyl) ethylenediamine), which is a common Zn^{2+} chelator for sequestration of intracellular zinc ions (Figure 6e, columns c and d). It should be noticed that the lysosomal Ca^{2+}, which is much higher than cytosolic calcium level, may result in potential interference on the Zn^{2+}-binding of TPEN (Log*K* [CaTPEN] = 4.4). To address this problem, we made another selectivity experiment (Figure S9) and found that 1 mM Ca^{2+} does not induce obvious influence on the coordination between Zn^{2+} and **DQZn4** or TPEN. Therefore, the increase in the ratio of

dx.doi.org/10.1021/ic301307v | *Inorg. Chem.* 2012, 51, 10842–10849

emission is originated from coordination between **DQZn4** and Zn^{2+}. **DQZn4** can readily reveal the variation of lysosomal Zn^{2+} in living cells. We also stimulated the cells with NO donor *S*-nitrosocystein (SNOC) to trigger intracellular stored Zn^{2+} release (Figure 7a–e). The ratio values gradually increased upon the stimulation and decreased rapidly after subsequent treatment with TPEN (Figure 7f). These data clearly establish that **DQZn4** is capable of detecting lysosomal Zn^{2+} changes after endogenous Zn^{2+} release with very high sensitivity. Considering that the significant roles of Zn^{2+} in lysosome function, autophagy, and neurological diseases have just been emphasized,[8,9] we anticipate that this lysosome-specific and ratiometric probe can contribute a useful molecular tool for the investigations on these processes.

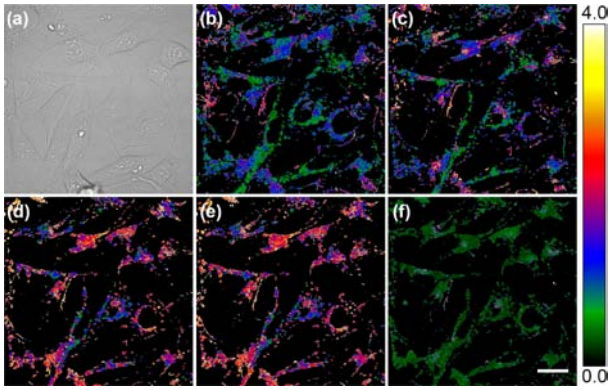

Figure 7. Ratiometric imaging of Zn^{2+} in **DQZn4**-labeled NIH 3T3 cells. (a) Bright-field image. (b–e) The cells were treated with SNOC (100 μM) for 0, 5, 20, and 25 min. (f) The cells were further treated with TPEN (50 μM) for 10 min. λ_{ex} = 405 nm, the ratio (F_{green}/F_{red}) was calculated as $Em_{430-510}/Em_{520-620\ nm}$. Scale bar: 20 μm; ratio bar: 0–4.

CONCLUSION

In summary, we designed and synthesized **DQZn4** as a ratiometric fluorescent probe with a nanomolar level K_d (16 nM) toward Zn^{2+} in acidic aqueous solution. This probe also exhibits high selectivity for Zn^{2+} over biological abundant Na^+, K^+, Ca^{2+}, and Mg^{2+}. As a targetable probe, we find that **DQZn4** can be easily loaded into cells for ratiometric detection of lysosomal Zn^{2+} changes in the presence of exogenous or endogenous Zn^{2+}. This design strategy, combining a selected chemical group as the targeting tag with a ratiometric sensing scaffold as the signal reporter, provides a simple and efficient method for ratiometric detection of subcellular zinc without any complex genetic-encoding procedures. The versatility of targeting groups for other subcellular domains and improvement of ratiometric sensing properties for Zn^{2+} are currently under construction.

EXPERIMENTAL SECTION

Materials and Methods. Unless otherwise noted, the chemicals were purchased from Alfa Aesar (China) or Sigma-Aldrich (China) and used as received. LysoTracker Red DND-99 was purchased from Invitrogen. All solvents were purified and dried by standard methods prior to use. Pure water (18.2 Ω) was used to prepare all aqueous solutions. Melting points were measured using an X-4 melting-point apparatus with a microscope. ^{1}H NMR and ^{13}C NMR spectra were recorded on a Bruker Avance-400 400 MHz spectrometer. All chemical shifts are reported in the standard notation of parts per million using residual solvent protons as internal standard. High resolution mass spectra (ESI) were obtained on a Bruker Apex IV Fourier transform mass spectrometer. UV–vis absorption spectra were obtained using a Hitachi 3010 UV–vis spectrometer. Fluorescence spectra were obtained using a Hitachi F-4600 spectrometer. Compound **1** was prepared from the known procedures.[19]

General Method for Synthetic Procedure for 2 and 7. A mixture of compound **1** (1.24 g, 5 mmol), alkyl chloride (10 mmol), K_2CO_3 (1.38 g, 10 mmol), and DMF (30 mL) under argon was stirred at 80 °C for 8 h. After the mixtured cooled, H_2O (30 mL) was added to the mixture and extracted with CH_2Cl_2 (20 mL × 3). The organic solutions were combined, washed with brine, and dried with Na_2SO_4. The solvents were evaporated to give the crude products, which were purified by flash chromatography (silica gel).

Compound ***2***. Chromatography (CH_2Cl_2/0–5% ethyl acetate). White solid. Yield 1.33 g (88%). Mp 144–145 °C. ^{1}H NMR (400 MHz, $CDCl_3$, ppm): δ 9.11 (d, J = 1.78 Hz, 1H), 8.48 (q, J_1 = 9.25 Hz, J_2 = 1.95 Hz, 1H), 8.30 (d, J = 9.27 Hz, 1H), 7.62 (s, 1H), 4.10–4.07 (m, 5H), 2.33 (s, 1H), 1.16 (d, J = 6.70 Hz, 6H). ^{13}C NMR (100 MHz, $CDCl_3$, ppm): δ 165.6, 164.4, 152.4, 150.7, 146.1, 132.0, 124.0, 121.6, 119.3, 102.3, 76.0, 53.7, 28.2, 19.3. ESI-HRMS: calcd for [M + H^+] $C_{15}H_{17}N_2O_5$, 305.1137; found, 305.1133.

Compound ***7***. Chromatography (CH_2Cl_2/0–5% ethyl acetate). White solid. Yield 1.45 g (80%). Mp 144–145 °C. ^{1}H NMR (400 MHz, $CDCl_3$, ppm): δ 9.13 (d, J = 2 Hz, 1H), 8.52 (q, J_1 = 9.20 Hz, J_2 = 2.4 Hz, 1H), 8.35 (d, J = 9.20 Hz, 1H), 7.68 (s, 1H), 4.44 (t, J = 6 Hz, 2H), 4.22 (q, J = 7.2 Hz, 2H), 4.10 (s, 3H), 2.65 (t, J = 6.8 Hz, 2H), 2.39 (m, 2H), 1.29 (q, J = 6.8 Hz, 3H). ^{13}C NMR (100 MHz, $CDCl_3$, ppm): δ 172.6, 165.4, 163.9, 152.3, 150.5, 146.0, 132.0, 124.0, 121.4, 119.2, 102.2, 68.8, 60.8, 53.6, 30.6, 24.0, 14.2. ESI-HRMS. calcd for [M + H^+] $C_{17}H_{19}N_2O_7$, 363.1192; found, 363.1187. [M + Na^+] $C_{17}H_{18}N_2NaO_7$, 385.1012; found, 385.1009.

General Method for Synthetic Procedure for 3 and 8. The compound **2** or **7** (5 mmol) and 10% Pd/C (0.20 g) were stirred in ethyl acetate (50 mL) under hydrogen gas at 25 °C for 8 h. The solution was filtered through Celite, and the solvent was evaporated. The products were characterized by ^{1}H NMR and HRMS-ESI, and used without further purification.

Compound ***3***. Yellow solid. Quantitative yield. Mp 164–165 °C. ^{1}H NMR (400 MHz, $CDCl_3$, ppm): δ 8.03 (d, J = 8.96 Hz, 1H), 7.46 (s, 1H), 7.29 (s, 1H), 7.18 (q, J_1 = 8.96 Hz, J_2 = 2.24 Hz, 1H), 4.12 (br, 2H), 4.04 (s, 3H), 4.00 (d, J = 6.44 Hz, 2H), 2.26 (m, 1H), 1.12 (d, J = 6.72 Hz, 6H). ESI-HRMS calcd for [M + H^+]: $C_{15}H_{19}N_2O_3$, 275.1396; found, 275.1389.

Compound ***8***. Yellow solid. Quantitative yield. Mp 214–215 °C. ^{1}H NMR (400 MHz, DMSO-d_6, ppm): δ 7.76 (d, J = 8.8 Hz, 1H), 7.33 (s, 1H), 7.21 (q, J_1 = 8.8 Hz, J_2 = 2.4 Hz, 1H), 7.06 (d, J = 2.4 Hz, 1H), 5.98 (s, 2H), 4.28 (t, J = 6 Hz, 2H), 4.11 (q, J = 7.2 Hz, 2H), 3.88 (s, 3H), 2.59 (t, J = 6.8 Hz, 2H), 2.14 (m, 2H), 1.20 (q, J = 7.2 Hz, 3H). ESI-HRMS: calcd for [M + H^+]: $C_{17}H_{21}N_2O_5$, 333.1450; found, 333.1446.

General Method for Synthetic Procedure for 4 and 9. A mixture of the amino **3** or **8** (1 mmol), paraformaldehyde (0.6 g), and sodium cyanoborohydride (0.19 g, 3 mmol) in acetic acid (20 mL) was stirred at the ambient temperature for 12 h. The solution was neutralized using excess $NaHCO_3$, and extracted in CH_2Cl_2 (3 × 50 mL). The organic solutions were washed with brine and dried with Na_2SO_4. The solvents were evaporated to give the crude products, which were purified by flash chromatography (silica gel).

Compound ***4***. Chromatography (CH_2Cl_2/0–20% ethyl acetate). Yellow solid. Yield 0.28 g (92%). Mp 128–129 °C. ^{1}H NMR (400 MHz, $CDCl_3$, ppm): δ 8.08 (d, J = 9.36 Hz, 1H), 7.47 (s, 1H), 7.37 (d, J = 9.32 Hz, 1H), 7.16 (d, J = 2.00 Hz, 1H), 4.04–4.02 (m, 5H), 3.12 (s, 6H), 2.29 (m, 1H), 1.14 (d, J = 6.68 Hz, 6H). ^{13}C NMR (100 MHz, $CDCl_3$, ppm): δ 166.7, 160.4, 149.3, 144.2, 141.9, 131.2, 124.0, 119.3, 100.7, 98.4, 74.7, 52.9, 40.4, 28.2, 19.3. ESI-HRMS: calcd for [M + H^+] $C_{17}H_{23}N_2O_3$, 303.1709; found, 303.1701.

Compound ***9***. Chromatography (CH_2Cl_2/0–20% ethyl acetate). Yellow oil. Yield 0.32 g (90%). ^{1}H NMR (400 MHz, $CDCl_3$, ppm): δ 8.05 (d, J = 9.6 Hz, 1H), 7.45 (s, 1H), 7.35 (q, J_1 = 9.6 Hz, J_2 = 2.8 Hz,

1H), 7.07 (d, J = 2.8 Hz, 1H), 4.30 (t, J = 6 Hz, 2H), 4.13 (q, J = 6.8 Hz, 2H), 4.01 (s, 3H), 3.09 (s, 6H), 2.59 (t, J = 7.2 Hz, 2H), 2.27 (m, 2H), 1.23 (q, J = 7.2 Hz, 3H). ^{13}C NMR (100 MHz, $CDCl_3$, ppm): δ 173.0, 166.7, 160.2, 149.5, 144.2, 142.0, 131.3, 123.9, 119.5, 100.8, 98.5, 67.6, 60.6, 53.0, 40.5, 31.0, 24.4, 14.3. ESI-HRMS: calcd for [M + H$^+$] $C_{19}H_{25}N_2O_5$, 361.1763; found, 361.1758.

General Method for Synthetic Procedure for 5 and 10. A mixture of **4** or **9** (1 mmol), and $NaBH_4$ (0.14 g, 4 mmol) in THF (20 mL) was stirred at 65 °C for 10 min. After that, methanol (10 mL) was added dropwise until **4** or **9** was completely reacted (TLC monitoring). The mixture was cooled to room temperature and then evaporated. After adding CH_2Cl_2 (20 mL), the solutions were washed with brine, and dried over Na_2SO_4. The solvent was evaporated to give crude products, which were purified by flash chromatography (silica gel).

Compound ***5***. Chromatography (CH_2Cl_2/1% $NH_3{\cdot}H_2O$/0−0.5% MeOH). White solid. Yield 0.23 g (85%). Mp 104−105 °C. ^{1}H NMR (400 MHz, $CDCl_3$, ppm): δ 7.86 (d, J = 9.20 Hz, 1H), 7.33 (d, J = 9.26 Hz, 1H), 7.21 (s, 1H), 6.51 (s, 1H), 4.78 (s, 2H), 4.39 (br, 1H), 3.94 (d, J = 6.46 Hz, 2H), 3.07 (s, 6H), 2.28 (m, 1H), 1.13 (d, J = 6.68 Hz, 6H). ^{13}C NMR (100 MHz, $CDCl_3$, ppm): δ 161.0, 156.2, 148.3, 141.4, 128.9, 122.2, 119.4, 100.3, 97.6, 74.6, 64.5, 40.9, 28.3, 19.4. ESI-HRMS: calcd for [M + H$^+$] $C_{16}H_{23}N_2O_2$, 275.1760; found, 275.1751.

Compound ***10***. Chromatography (CH_2Cl_2/1% $NH_3{\cdot}H_2O$/0−1% EtOH). White solid. Yield 0.20 g (61%). Mp 58−59 °C. ^{1}H NMR (400 MHz, $CDCl_3$, ppm): δ 7.87 (d, J = 9.2 Hz, 1H), 7.34 (q, J_1 = 9.2 Hz, J_2 = 2.8 Hz, 1H), 7.16 (d, J = 2.8 Hz, 1H), 6.53 (s, 1H), 4.79 (s, 2H), 4.25 (t, J = 6 Hz, 2H), 4.18 (q, J = 7.2 Hz, 2H), 3.08 (s, 6H), 2.61 (t, J = 7.2 Hz, 2H), 2.0 (m, 2H), 1.26 (q, J = 7.2 Hz, 3H). ^{13}C NMR (100 MHz, $CDCl_3$, ppm): δ 173.1, 160.5, 156.4, 148.3, 141.5, 128.8, 121.9, 119.4, 100.1, 97.7, 67.3, 64.4, 60.7, 40.9, 30.9, 24.4, 14.3. ESI-HRMS: calcd for [M + H$^+$]: $C_{18}H_{25}N_2O_4$, 333.1814; found, 333.1810.

General Method for Synthetic Procedure for 6 and 11. A solution of **5** or **10** (1 mmol) was stirred in dry methylene chloride (30 mL) at room temperature with 1.0 g of manganese dioxide. After 8 h, the mixture was filtered off. The solvent was evaporated to give crude products, which were purified by flash chromatography (silica gel).

Compound ***6***. Chromatography (CH_2Cl_2/0−20% ethyl acetate). Yellow solid. Yield 0.25 g (92%). Mp 140−141 °C. ^{1}H NMR (400 MHz, $CDCl_3$, ppm): δ 10.11 (s, 1H), 8.05 (br, 1H), 7.41 (q, J_1 = 9.16 Hz, J_2 = 2.40 Hz, 1H), 7.29 (s, 1H), 7.17 (d, J = 2.52 Hz, 1H), 4.05 (d, J = 6.48 Hz, 2H), 3.16 (s, 6H), 2.29 (m, 1H), 1.14 (d, J = 6.68 Hz, 6H). ^{13}C NMR (100 MHz, $CDCl_3$, ppm): δ 194.1, 160.6, 150.4, 150.0, 142.5, 131.1, 125.1, 119.4, 99.0, 96.8, 74.9, 40.6, 29.8, 28.3, 19.4. ESI-HRMS: calcd for [M + H$^+$]: $C_{16}H_{21}N_2O_2$, 273.1603; found, 273.1590.

Compound ***11***. Chromatography (CH_2Cl_2/0−20% ethyl acetate). Yellow solid. Yield 0.31 g (94%). Mp 91−92 °C. ^{1}H NMR (400 MHz, $CDCl_3$, ppm): δ 10.06 (s, 1H), 8.02 (d, J = 9.2 Hz, 1H), 7.40 (q, J_1 = 9.6 Hz, J_2 = 3.2 Hz, 1H), 7.28 (s, 1H), 7.12 (d, J = 2.8 Hz, 1H), 4.33 (t, J = 6.4 Hz, 2H), 4.16 (q, J = 7.2 Hz, 2H), 3.16 (s, 6H), 2.59 (t, J = 7.2 Hz, 2H), 2.30 (m, 2H), 1.26 (q, J = 7.2 Hz, 3H). ^{13}C NMR (100 MHz, $CDCl_3$, ppm): δ 193.9, 172.9, 160.1, 150.1, 150.0, 142.4, 131.1, 124.9, 119.4, 98.8, 96.7, 67.7, 60.7, 40.5, 31.0, 24.4, 14.3. ESI-HRMS: calcd for [M + H$^+$]: $C_{18}H_{23}N_2O_4$, 331.1658; found, 331.1654. [M + Na$^+$]: $C_{18}H_{22}N_2NaO_4$, 353.1477; found, 353.1474.

General Method for Synthetic Procedure DQZn3 and 12. To a solution of **6** or **11** (0.5 mmol), and DPA (0.1 g, 0.5 mmol) in 1,2-dichloroethane (10 mL), $NaBH(OAc)_3$ (0.13 g, 0.6 mmol) was added in portions. The resulting solution was stirred at room temperature overnight. Then the solvent was evaporated, and the solids were diluted with CH_2Cl_2, washed with brine, and dried over Na_2SO_4. The solvents were evaporated to give crude products which were purified by flash chromatography (silica gel).

DQZn3. Chromatography (CH_2Cl_2/1% $NH_3{\cdot}H_2O$/0−1% MeOH). Yellow oil. Yield 0.21 g (93%). ^{1}H NMR (400 MHz, DMSO, ppm): δ 8.51 (d, J = 4.48 Hz, 2H), 7.80−7.76 (m, 2H), 7.72 (d, J = 9.24 Hz, 1H), 7.62 (d, J = 7.76 Hz, 2H), 7.38 (q, J_1 = 9.28 Hz, J_2 = 2.76 Hz, 1H), 7.27 (m, 2H), 7.11 (s, 1H), 7.03 (d, J = 2.64 Hz, 1H), 3.99 (d, J = 6.44 Hz, 2H), 3.82 (s, 6H), 2.99 (s, 6H), 2.19 (m, 1H), 1.08 (d, J = 6.68 Hz, 6H). ^{13}C NMR (100 MHz, $CDCl_3$, ppm): δ 160.4, 159.2, 156.7, 148.9, 147.8, 142.0, 136.0, 128.9, 122.9, 121.7, 121.6, 118.8, 100.0, 99.6, 74.1, 60.9, 59.9, 40.6, 27.9, 19.2. ESI-HRMS: calcd for [M + H$^+$]: $C_{28}H_{34}N_5O$, 456.2763; found, 456.2745.

Compound ***12***. Chromatography (CH_2Cl_2/1% $NH_3{\cdot}H_2O$/0−1% EtOH). Yield 0.22 g (85%). ^{1}H NMR (400 MHz, $CDCl_3$, ppm): δ 8.56 (d, J = 4.40 Hz, 2H), 7.85 (d, J = 9.2 Hz, 1H), 7.64 (t, J = 7.6 Hz, 2H), 7.57 (d, J = 7.6 Hz, 2H), 7.28 (q, J_1 = 9.2 Hz, J_2 = 2.8 Hz, 1H), 7.15−7.12 (m, 4H), 4.30 (t, J = 6.0 Hz, 2H), 4.18 (q, J = 7.2 Hz, 2H), 3.94 (s, 2H), 3.92 (s, 4H), 3.05 (s, 6H), 2.63 (t, J = 7.2 Hz, 2H), 2.31 (m, 2H), 1.26 (q, J = 6.8 Hz, 3H). ^{13}C NMR (100 MHz, $CDCl_3$, ppm): δ 172.8, 160.1, 159.1, 156.6, 148.9, 147.9, 142.0, 136.2, 128.9, 123.1, 121.8, 121.5, 118.9, 100.1, 99.6, 66.9, 61.0, 60.3, 60.0, 40.6, 30.7, 24.2, 14.0. ESI-HRMS calcd for [M + H$^+$]: $C_{30}H_{36}N_5O_3$, 514.2818; found, 514.2826.

DQZn4. Compound **12** (0.31 g, 0.5 mmol) was dissolved in a mixture of MeOH (20 mL) and H_2O (4 mL). NaOH (5 equiv) was added, and the solution was stirred at ambient temperature for 20 h. The solution was neutralized using excess HCl (0.1 M) and the product was extracted with CH_2Cl_2. The organic phase was washed with water, dried over Na_2SO_4, and evaporated to give yellow solids, which were used without further purification. These solids (carboxylic acid) were stirred with oxalyl chloride (3 equiv) in anhydrous CH_2Cl_2 (20 mL) at room temperature for 4 h. After evaporating the solvent, the acid chloride was dissolved in anhydrous CH_2Cl_2 (10 mL), then a solution of *N*,*N*-dimethylethane-1,2-diamine and diisopropylethylamine (5.5 equiv) in anhydrous CH_2Cl_2 (10 mL) was slowly added. The reaction mixture was allowed to stir at room temperature for 1 h. The solvent was then removed and the residue was purified by flash chromatography on silica gel eluting with CH_2Cl_2/1% $NH_3{\cdot}H_2O$/0−1% MeOH, to afford the pure products. Yellow oil. Yield 0.13 g (46%). ^{1}H NMR (400 MHz, $CDCl_3$, ppm): δ 8.54 (d, J = 4.40 Hz, 2H), 7.85 (d, J = 9.6 Hz, 1H), 7.67 (t, J = 7.6 Hz, 2H), 7.57 (d, J = 7.6 Hz, 2H), 7.31 (q, J_1 = 9.6 Hz, J_2 = 3.2 Hz, 1H), 7.14−7.08 (m, 4H), 6.12 (s, 1H), 4.28 (t, J = 5.6 Hz, 2H), 3.93 (s, 2H), 3.91 (s, 4H), 3.30 (q, J = 5.6 Hz, 2H), 3.06 (s, 6H), 2.50 (t, J = 7.2 Hz, 2H), 2.33 (m, 4H), 2.09 (s, 6H). ^{13}C NMR (100 MHz, $CDCl_3$, ppm): δ 172.2, 160.4, 159.4, 156.9, 149.1, 148.1, 142.3, 136.4, 129.2, 123.2, 122.0, 121.7, 119.1, 100.3, 99.8, 67.3, 61.2, 60.2, 57.8, 45.0, 40.9, 36.8, 32.9, 25. ESI-HRMS: calcd for [M + H$^+$] $C_{32}H_{42}N_7O_2$, 556.3400; found, 556.3405. [M + Na$^+$] $C_{32}H_{41}N_7NaO_2$, 578.3219; found, 578.3230.

Determination of Protonation Constants. The apparent pK_a was measured by plotting the emission intensity at selected wavelength vs pH recorded in the range from pH ∼2 to ∼11. A solution of **DQZn3** or **DQZn4** was acidified by adding HCl (6 N), and the fluorescence spectra (5 μM) were recorded. Aliquots of 6, 3, 1, 0.5, and 0.1 N NaOH were added to achieve appropriate pH changes (ΔpH = 0.3−0.5), and the fluorescence spectra were recorded after each addition. The overall volume change for each experiment did not exceed ∼2%. Throughout the titration, the temperature was maintained at 25 ± 0.5 °C by circulating constant-temperature water through the water-jacket of the titration cell. The resulting fluorescence emission intensity (F) was plotted as a function of pH and fitted to the expression in eq 1[20] to calculate the pK_a values. ΔF_1 and ΔF_2 are the maximum fluorescence emission intensity changes associated with the corresponding pK_a values.

$$\Delta F = \frac{\Delta F_1}{1 + 10^{(pH - pK_{a1})}} + \frac{\Delta F_2}{1 + 10^{(pH - pK_{a2})}} \quad (1)$$

Determination of Dissociation Constant. Fluorescence intensity ratio values of 5 μM **DQZn3** and **DQZn4** as a function of free zinc ion concentration were measured in HEPES buffer solution (10 mM HEPES, 0.1 M NaCl, 2 mM NTA, pH = 7.4) and MES buffer solution (20 mM MES, 0.1 M NaCl, 2 mM NTA, pH = 5.2). The log$K$ and pK_a values of nitrilotriacetic acid (NTA) were taken from the literature (log$K$ (Zn-NTA) = 10.66 (25 °C, I = 0.1) and pK_{a1} = 9.65, pK_{a2} = 2.48, pK_{a3} = 1.8).[21] Protonation constants must be corrected upward by 0.11 when working at 0.1 M ionic strength. Free Zn^{2+} concentration

dx.doi.org/10.1021/ic301307v | Inorg. Chem. 2012, 51, 10842−10849

was calculated using the method described in the literature.[22] The solutions were allowed to equilibrate at 25 ± 0.5 °C for 5 min after each addition. The ratio values were plotted and fitted to the following eqs 3 and 4 as described.[23]

$$R(\lambda_{em}^{1}/\lambda_{em}^{2}) = \frac{[M^{2+}]_{free}R_{max} + K_d\xi R_{min}}{K_d\xi + [M^{2+}]_{free}} \quad (3)$$

$$\xi = \frac{F_{min}(\lambda_{em}^{2})}{F_{max}(\lambda_{em}^{2})} \quad (4)$$

Metal Ion Selectivity. The fluorescence spectra of a 2-mL aliquot of 5 μM **DQZn4** were acquired in MES buffer solution after addition of an aliquot of metal stock solutions. The final concentrations of the metal ions are 1.0 mM for KNO_3, $Mg(NO_3)_2$, $Ca(NO_3)_2$, and 5 μM for $MnCl_2$, $FeSO_4$ (newly prepared), $Co(NO_3)_2$, $NiSO_4$, $Cu(NO_3)_2$, and $Cd(ClO_4)_2$. After acquisitions, an aliquot of $ZnSO_4$ (5 μM) was further titrated into relevant solutions, and the fluorescence of competing samples were measured again. Excitation was provided at 405 nm, and the emission intensity ratio was calculated as $F_{495\ nm}/F_{542\ nm}$.

Cell Culture. NIH 3T3 cells were cultured in Dulbecco's modified Eagle's medium (DMEM, Gibco) supplemented with 10% fetal calf serum (FCS, Gibco), 50 μg/mL penicillin/streptomycin (Hyclone) at 37 °C in a 5/95 CO_2/air incubator. The cells were cultured for 2 days before dye-loading on a 35-mm diameter glass-bottomed coverslip.

Fluorescence Imaging. Confocal fluorescence imaging experiments were performed on an Olympus FV-1000 laser scanning microscopy system, based on an IX81 (Olympus, Japan) inverted microscope. The microscope was equipped with multiple visible laser lines (405, 458, 488, 515, 543, 635 nm, CW) and UPLSAPO 60×/N.A 1.42 objective. Images were collected and processed with Olympus FV10-ASW software (Ver. 2.1b).

For colocalization experiments: 10 μM **DQZn4**, and 1 μM Lysotracker Red DND-99 in the serum-free DMEM were added to the cells, and the cells were incubated at 37 °C for 30 min. After washing with phosphate-buffered saline (PBS, 2 mL × 3) to remove the dyes, the cells were filled with 2 mL of PBS for fluorescence imaging on a FV1000 confocal laser-scanning microscope equipped with the appropriate excitation and emission filters for **DQZn4** (λ_{ex} = 405 nm, λ_{em} = 450−510 nm), Lysotracker Red (λ_{ex} = 543 nm, λ_{em} = 560−660 nm). The Pearson's colocalization coefficient between the channels was measured by using FV10-ASW software (Ver. 2.1b).

For ratiometric imaging of intracellular Zn^{2+}, 10 μM **DQZn4** (2.5 mM stock solution) in the culture media containing 0.4% (v/v) DMSO was added to the cells. The cells were incubated at 37 °C for 30 min, and washed with PBS three times to remove the excess probe and bathed in PBS (2 mL) before imaging. After washing with PBS (2 mL × 3) to remove the excess probe, the cells were treated with 30 μM $ZnSO_4$ and 15 μM pyrithione for 5 min, or 100 μM SNOC for 25 min in PBS. Subsequent treatment with 50 μM TPEN (*N*,*N*,*N*′,*N*′-tetrakis(2-pyridylmethyl)ethylenediamine) was performed directly on the microscope stage. Fluorescence at two emission channels of 430−510 nm (green) and 520−620 nm (red) for **DQZn4** were measured at 25 °C by exciting at 405 nm. The ratio images of F_{green}/F_{red} were processed on a pixel-by-pixel basis using FV10-ASW software (Ver. 2.1b).

■ ASSOCIATED CONTENT

Supporting Information

Additional spectroscopic data for **DQZn3** and **DQZn4**, and intracellular imaging data. This material is available free of charge via the Internet at http://pubs.acs.org.

■ AUTHOR INFORMATION

Corresponding Author

*E-mail: hjiang@iccas.ac.cn.

Notes

The authors declare no competing financial interest.

■ ACKNOWLEDGMENTS

We thank the National Natural Science Foundation of China (21102148, 21125205), National Basic Research Program of China (2009CB930802, 2011CB935800), and the Key Laboratory of Pesticide & Chemical Biology, Ministry of Education, Central China Normal University for financial support.

■ REFERENCES

(1) (a) Jiang, P. J.; Guo, Z. J. *Coord. Chem. Rev.* **2004**, *248*, 205−229. (b) Kikuchi, K.; Komatsu, K.; Nagano, T. *Curr. Opin. Chem. Biol.* **2004**, *8*, 182−191. (c) Domaille, D. W.; Que, E. L.; Chang, C. J. *Nat. Chem. Biol.* **2008**, *4*, 168−175. (d) Tomat, E.; Lippard, S. J. *Curr. Opin. Chem. Biol.* **2010**, *14*, 225−230.

(2) (a) Xie, X.; Smart, T. G. *Nature* **1991**, *349*, 521−524. (b) Berg, J. M.; Shi, Y. *Science* **1996**, *271*, 1081−1085.

(3) (a) Eide, D. J. *Biochim. Biophys. Acta* **2006**, *1763*, 711−722. (b) Kröncke, K.-D. *Arch. Biochem. Biophys.* **2007**, *463*, 183−187. (c) Rink, L.; Haase, H. *Trends Immunol.* **2007**, *28*, 1−4. (d) Murakami., M.; Hirano., T. *Cancer Sci* **2008**, *99*, 1515−1522. (e) Kehl-Fie, T. E.; Skaar, E. P. *Curr. Opin. Chem. Biol.* **2010**, *14*, 218−224.

(4) Tomat, E.; Nolan, E. M.; Jaworski, J.; Lippard., S. J. *J. Am. Chem. Soc.* **2008**, *130*, 15776−15777.

(5) (a) Keppler, A.; Gendreizig, S.; Gronemeyer, T.; Pick, H.; Vogel, H.; Johnsson, K. *Nat. Biotechnol.* **2003**, *21*, 86−89. (b) Gautier, A.; Juillerat, A.; Heinis, C.; Correa, I. R.; Kindermann, M.; Beaufils, F.; Johnsson, K. *Chem. Biol.* **2008**, *15*, 128−136. (c) Los, G. V.; et al. *ACS Chem. Biol.* **2008**, *3*, 373−382. (d) Srikun, D.; Albers, A. E.; Nam, C. I.; Iavarone, A. T.; Chang., C. J. *J. Am. Chem. Soc.* **2010**, *132*, 4455−4465.

(6) (a) Shynkar, V. V.; Klymchenko, A. S.; Kunzelmann, C.; Duportail, G.; Muller, C. D.; Demchenko, A. P.; Freyssinet, J.-M.; Mely, Y. *J. Am. Chem. Soc.* **2007**, *129*, 2187−2193. (b) Freundt, E. C.; Czapiga, M.; Lenardo, M. J. *Cell Res.* **2007**, *17*, 956−958. (c) Kim, H. M.; An, M. J.; Hong, J. H.; Jeong, B. H.; Kwon, O.; Hyon, J. Y.; Hong, S. C.; Lee, K. J.; Cho, B. R. *Angew. Chem., Int. Ed.* **2008**, *47*, 2231−2234. (d) Kim, H. M.; Jeong, B. H.; Hyon, J. Y.; An, M. J.; Seo, M. S.; Hong, J. H.; Lee, K. J.; Kim, C. H.; Joo, T.; Hong, S. C.; Cho, B. R. *J. Am. Chem. Soc.* **2008**, *130*, 4246−4247. (e) Dickinson, B. C.; Srikun, D.; Chang, C. J. *Curr. Opin. Chem. Biol.* **2010**, *14*, 50−56. (f) Son, J. H.; Lim, C. S.; Han, J. H.; Danish, I. A.; Kim, H. M.; Cho, B. R. *J. Org. Chem.* **2011**, *76*, 8113−8116. (g) Lee, M. H.; Han, J. H.; Kwon, P.-S.; Bhuniya, S.; Kim, J. Y.; Sessler, J. L.; Kang, C.; Kim, J. S. *J. Am. Chem. Soc.* **2012**, *134*, 1316−1322.

(7) Lee, S. J.; Koh, J. Y. *Mol. Brain* **2010**, *3*, 30−39.

(8) (a) Lee, S. J.; Cho, K. S.; Koh, J. Y. *Glia* **2009**, *57*, 1351−1361. (b) Lee, S. J.; Park, M. A.; KIM, H. J.; Koh, J. Y. *Glia* **2010**, *58*, 1186−1196.

(9) (a) Sensi, S. L.; Ton-That, D.; Weiss, J. H.; Rothe, A.; Gee, K. R. *Cell Calcium* **2003**, *34*, 281−284. (b) Vinkenborg, J. L.; Nicolson, T. J.; Bellomo, E. A.; Koay, M. S.; Rutter, G. A.; Merkx, M. *Nat Methods* **2009**, *6*, 737−740. (c) Dittmer, P. J.; Miranda, J. G.; Gorski, J. A.; Palmer, A. E. *J. Biol. Chem.* **2009**, *284*, 16289−16297. (d) Qin, Y.; Dittmer, P. J.; Park, J. G.; Jansen, K. B.; Palmer, A. E. *Proc. Natl. Acad. Sci., U.S.A.* **2011**, *108*, 7351−7356. (e) Masanta, G.; Lim, C. S.; Kim, H. J.; Han, J. H.; Kim, H. M.; Cho, B. R. *J. Am. Chem. Soc.* **2011**, *133*, 5698−5700. (f) Iyoshi, S.; Taki, M.; Yamamoto, Y. *Org. Lett.* **2011**, *13*, 4558−4561. (g) Baek, N. Y.; Heo, C. H.; Lim, C. S.; Masanta, G.; Cho, B. R.; Kim, H. M. *Chem. Commun.* **2012**, *48*, 4546−4548. (h) Xue, L.; Li, G. P.; Yu, C. L.; Jiang, H. *Chem.—Eur. J.* **2012**, *18*, 1050−1054. (i) Liu, Z. P.; Zhang, C. L.; Chen, Y. C.; He, W. J.; Guo, Z. J. *Chem. Commun.* **2012**, *48*, 8365−8367.

(10) (a) Grynkiewicz, G.; Poenie, M.; Tsien, R. Y. *J. Biol. Chem.* **1985**, *260*, 3440−3450. (b) Dunn, K. W.; Mayor, S.; Myers, J. N.; Maxfield, F. R. *FASEB J.* **1994**, *8*, 573−582.

(11) Selected reviews: (a) Lim, N. C.; Freake, H. C.; Brückner, C. *Chem.—Eur. J.* **2005**, *11*, 38−49. (b) Dai, Z.; Canary, J. W. *New J. Chem.* **2007**, *31*, 1708−1718. (c) Carol, P.; Sreejith, P.; Ajayaghosh, A. *Chem. Asian J.* **2007**, *2*, 338−348. (d) Que, E. L.; Domaille, D. W.; Chang, C. J. *Chem. Rev.* **2008**, *108*, 1517−1549. (e) Xu, Z.; Yoon., J.; Spring, D. R. *Chem. Soc. Rev.* **2010**, *39*, 1996−2006. (f) Vinkenborga, J. L.; Koaya, M. S.; Merkx., M. *Curr. Opin. Chem. Biol.* **2010**, *14*, 231−237.
(12) (a) Xue, L.; Li, G. P.; Liu, Q.; Wang, H. H.; Liu, C.; Ding, X. L.; He, S. G.; Jiang, H. *Inorg. Chem.* **2011**, *50*, 3680−3690. (b) Wang, H. H.; Xue, L.; Jiang, H. *Org. Lett.* **2011**, *13*, 3844−3877.
(13) (a) Xue, L.; Liu, C.; Jiang, H. *Org. Lett.* **2009**, *11*, 1655−1658. (b) Xue, L.; Liu, Q.; Jiang, H. *Org. Lett.* **2009**, *11*, 3454−3457.
(14) Hall, H. K. *J. Am. Chem. Soc.* **1957**, *79*, 5441−5444.
(15) (a) Han, J.; Burgess., K. *Chem. Rev.* **2010**, *110*, 2709−2728. (b) Casey, J. R.; Grinstein, S.; Orlowski, J. *Nat. Rev. Mol. Cell Biol.* **2010**, *11*, 50−61.
(16) (a) Li, Y.; Hough, C. J.; Suh, S. W.; Sarvey, J. M.; Frederickson, C. J. *J. Neurophysiol.* **2001**, *86*, 2597−2604. (b) Li, Y.; Hough, C. J.; Frederickson, C. J.; Sarvey, J. M. *J. Neurosci.* **2001**, *21*, 8015−8025. (c) Bozym, R. A.; Thompson, R. B.; Stoddard, A. K.; Fierke, C. A. *ACS Chem. Biol.* **2006**, *1*, 103−111.
(17) (a) Hanaoka, K.; Kikuchi, K.; Kojima, H.; Urano, Y.; Nagano, T. *J. Am. Chem. Soc.* **2004**, *126*, 12470−12476. (b) Xue, L.; Wang, H. H.; Wang, X. J.; Jiang, H. *Inorg. Chem.* **2008**, *47*, 4310−4318. (c) Chen, X.-Y.; Shi, J.; Li, Y.-M.; Wang, F.-L.; Wu, X.; Guo, Q.-X.; Liu, L. *Org. Lett.* **2009**, *11*, 4426−4429. (d) Meng, X. M.; Wang, S. X.; Li, Y. M.; Zhu, M. Z.; Guo, Q. X. *Chem. Commun.* **2012**, *48*, 4196−4198.
(18) Manders, E. M. M.; Verbeek, F. J.; Aten, J. A. *J. Microsc.* **1993**, *169*, 375−382.
(19) Jaen, J. C.; Laborde, E.; Bucsh, R. A.; Caprathe, B. W.; Sorenson, R. J.; Fergus, J.; Spiegel, K.; Marks, J.; Dickerson, M. R.; Davis, R. E. *J. Med. Chem.* **1995**, *38*, 4439−4445.
(20) Burdette, S. C.; Walkup, G. K.; Spingler, B.; Tsien, R. Y.; Lippard, S. J. *J. Am. Chem. Soc.* **2001**, *123*, 7831−7841.
(21) Martell, A. E., Smith, R. M. *Critical Stability Constants, Vol. 1: Amino Acids*; Plenum Press: New York, 1974.
(22) Perrin, D. D.; Dempsy, B. *Buffers for pH and Metal Ion Control*; John Wiley & Sons, Chapman and Hall: New York, London, 1974.
(23) Cielen, E.; Stobiecka, E.; Tahri, A.; Hoornaert, G. J.; De Schryver, F. C.; Gallay, J.; Vincent, M.; Boens, N. *J. Chem. Soc., Perkin Trans. 2* **2002**, *2*, 1197−1206.